Non-linear fracture mechanics in LS-DYNA and LS-PrePost

Per Lindström[1, 2], Anders Jonsson[3], Anders Jernberg[3], Erling Østby[2]

[1] Department of Engineering Science, University West, Trollhättan, Sweden
[2]DNV GL Materials Laboratory, Høvik, Norway
[3]DYNAmore Nordic AB

1 Introduction

Fracture mechanics provides an engineering framework for assessing the consequences of defects in structures. In linear elastic fracture mechanics (LEFM), stress intensity factors K_I, K_{II} and K_{III} are used for characterizing the stress singularity at the crack tip, which arises from the theory of linear elasticity. Crack growth is assumed to occur when K_I exceeds the fracture toughness KC. LEFM can be useful for brittle materials, or when the size of the plastic zone is small compared to global dimensions (see for example Ref. [12]).
In non-linear fracture mechanics (EPFM), an energy based criterion is used for assessing the risk for crack growth: if the energy release rate at the crack tip exceeds what is required for creating new surfaces in the material, crack growth will occur. Under certain assumptions the energy release rate at the crack tip can be calculated by a path independent integral, the so-called *J*-integral [13]. In modern FE-based fracture mechanics applied to practical design, the structure under consideration is modelled, including cracks at specific locations, and the J-integral values are computed and used as design criteria. From a numerics viewpoint, the *J*-integral has many appealing properties: it can be evaluated from the far-field solution, which reduces numerical errors that may arise close to the crack tip, and the expected path-independence can to some extent be used as a quick check on solution validity.
Evaluation of the *J*-integral from LS-DYNA [7] simulation results has been implemented as a post-processing tool in LS-PrePost, including consistent treatment of residual stresses. The implementation covers both 2D (plane stress / plane strain) and 3D applications, using the virtual crack-tip extension (VCE) method. The tool is accessible both via the LS-PrePost GUI and via command file interface.

2 Theoretical background

The -integral can be derived as a conservation law for the energy momentum tensor, following for example Refs. [2][8], or from considering the energy flow to the crack tip, see for example Section 4.2 of Ref. [5]. The classical definition of *J* is due to Rice [13],

$$J = \int_{\Gamma} \left(W \mathrm{d}y - \mathbf{T} \bullet \frac{\partial \mathbf{u}}{dx} \mathrm{d}s \right), \tag{1}$$

where *W* is the strain energy density, $T_i = \sigma_{ij} n_j$ is the traction vector, and Γ is a curve counter-clockwise from the lower crack face to the upper, see Fig.1:. It can be shown that the *J*-integral will be independent of the curve Γ, under certain assumptions; the most important ones perhaps being that a homogeneous hyper-elastic material is considered, and that the crack faces are straight and traction free. The assumptions required for *J* to be path independent are discussed in detail in Ref. [2].

In order to evaluate the *J*-integral in a finite elements framework, it is very convenient to transform the contour integral to a surface integral. This can be done using the virtual crack extension (VCE) method [16], which can be seen as “virtual shift” (without altering the stress state) of the crack front in the crack direction, see the left image of Fig.1:. Mathematically, this involves the introduction of a smooth weighting function *q*, which is zero on Γ, and one on the crack front nodes and the interior of A. By use of the divergence theorem, this yields

$$J = -\frac{1}{\Delta A_c} \int_A \left(W \delta_{1i} - \sigma_{ij} u_{j,1} \right) q_{,i} \mathrm{d}A, \tag{2}$$

where ΔA_c is the virtual increase in crack area.

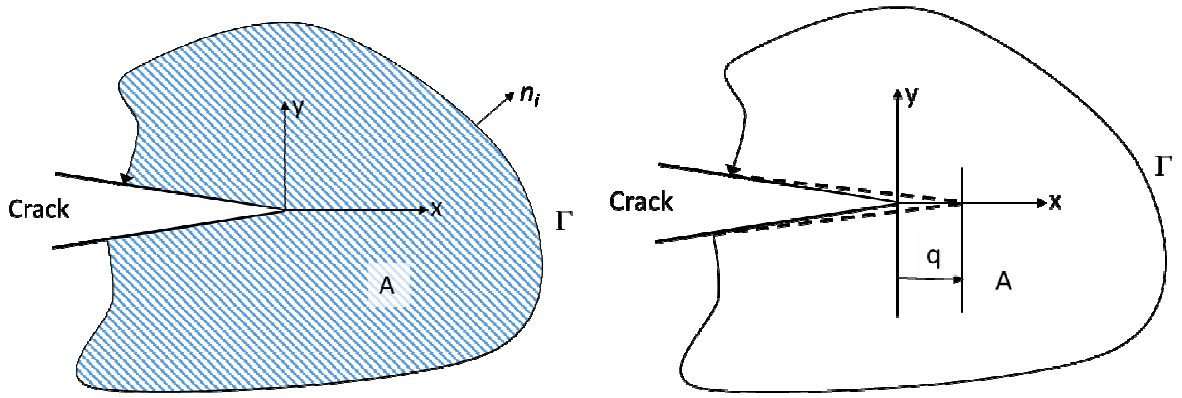

Fig.1: Definition of the curve Γ and the domain A for calculating the J-integral. The left image shows the virtual crack extension q.

The definition of a path-independent *J* can be extended to account for residual stresses [1], body forces, applied tractions on the crack faces and thermal stresses (see for example Eq. (6.47) of Ref. [14] for an extended *J*-integral formulation). Also inhomogeneous materials can be treated, see for example Ref. [15].

Under small scale yielding conditions, the *J*-integral is related to the stress intensity factors by [5]

$$J = \frac{K_I^2 + K_{II}^2}{E'} + \frac{(1+\nu)K_{III}^2}{E}. \tag{3}$$

It is also possible to relate the crack-tip opening displacement (CTOD) to *J* by [9]

$$J = m \cdot \sigma_Y \cdot CTOD, \tag{4}$$

where σ_Y is the yield strength of the material, and the proportionality factor *m* depends on crack geometry [10], material properties [19], and possibly also on the loading of the specimen [18].

3 Implementation in LS-PrePost

The computation of the *J*-integral was implemented as a post-processing tool in LS-PrePost, for bi-linear quad elements in 2D and bilinear hexahedra in 3D. The crack can have an arbitrary orientation, it must not be aligned to the global coordinate axes. For 3D geometries, both the global *J*, corresponding to a uniform virtual crack extension of the entire crack front, as well as the local *J* at each node of the crack front is presented.

In order to account for a state of residual stresses and strains, the method of Ref. [1] is used. This involves a modification of the strain energy density, to account for plastic work done when creating the residual state,

$$W = W^{\text{total}} - W^{\text{P}}_{\text{residual state}}, \tag{5}$$

where $W^{\text{P}}_{\text{residual state}}$ is the plastic work done when creating the residual state. In LS-DYNA, the residual state would most likely be represented by a **`dynain`** – file. However, the **`dynain`** file contains no information regarding energies, and the strain energy density in the subsequent analysis will be

$$W^* = W^{\text{total}} - W^{\text{total}}_{\text{residual state}}. \tag{6}$$

In order to obtain the desired modification of the strain energy density of Eq. (5), it is assumed that $W^{\text{total}} = W^e + W^p$ (no thermal loading) which makes it possible to express the desired form of *W* as

$$W = W^* + W^{\text{e}}_{\text{residual state}}, \tag{7}$$

and the elastic strain energy density W^e is computed as

$$W^e = \frac{1}{2}\sigma : \varepsilon^{\mathbf{e}} = \frac{1}{2}\sigma : (\mathbf{C}^{-1}\sigma), \tag{8}$$

where **C** is the elasticity tensor of the material. The *J*-integral definition of Ref. [1] also involves the initial strain $\boldsymbol{\varepsilon}^0$, which is computed in a similar way as in Eq. (8),

$$\varepsilon^0 = \left(\varepsilon - \varepsilon^{\mathbf{e}}\right)_{\text{initial state}} = \left(\varepsilon - \mathbf{C}^{-1}\sigma\right)_{\text{initial state}}. \tag{9}$$

It shall be noted that $\boldsymbol{\varepsilon}^0$ is constant in the subsequent analysis. By Eqs. (7) and (9), the *J*-integral of Ref. [1] can be evaluated as

$$J = -\frac{1}{\Delta A_c}\int_A \left[\left(W\delta_{1i} - \sigma_{ij}u_{j,1}\right)q_{,i} + \sigma_{ij}\varepsilon^0_{ij,1}q\right]\mathrm{d}A. \tag{10}$$

The numerical implementation, using iso-parametric shape functions and Gaussian quadrature, closely follows Refs. [1], [3] and [14]. In the **d3plot**-format, the strain filed is available only at the element centroid location. In order to overcome this, the nodal values of the initial strains $\boldsymbol{\varepsilon}^0$ are computed by averaging from the neighboring elements.

Effects of thermal loading, body forces or tractions on the crack faces are not included in the current implementation. Also the correct treatment of interfaces between different materials is currently not implemented.

3.1 Model requirements

The present implementation of the *J*-integral evaluation in LS-PrePost is a pure post-processing tool. The user need not make any special path definitions as output requests in advance in the LS-DYNA simulation. However, it is required to output the stresses, strains and internal energy from the simulation in the resulting d3plot - files. For solid elements, the internal energy can be output by setting HYDRO = 1 on ***DATABASE_EXTENT_BINARY**.
In traditional non-linear fracture mechanics, implicit quasi-static solutions have been used. In LS-DYNA / LS-PrePost, both implicit and explicit analyses can be used for computing *J*, but it shall be emphasized that the *J*-integral of Eq. (10) does not account for dynamic effects. In order to obtain a reasonably accurate *J* from an explicit LS-DYNA simulation, dynamic effects should be negligible.
The present *J*-integral evaluation has been implemented for quadrilateral 2D plane stress / plane strain elements and hexahedral 3D solid elements. For fracture mechanics analyses, a strictly structured mesh around the crack tip is almost always used, creating well-defined paths of elements for *J*-integral evaluation (see for example Fig.2:).

For FE fracture mechanics and fatigue analyses, it may be desired to use the smallest acceptable mesh size in the vicinity of the crack tip, in order to capture the stress singularity effect (LEFM-analyses) or the crack driving force (EPFM-analyses) respectively.
The smallest acceptable element size is limited by the continuum assumption of the material model. Metallic material models constructed on the basis of industrial standardized mechanical test results have validity on first order 3D element volumes containing not less than about 100 grains (5 × 5 × 5 grains or 4 × 4 × 4 grains). There the use of first order 3D elements volumes containing less than 64 grains may be acceptable for case by case considerations.
Typical grain size for fine grain steels are 10 – 20 µm and the grain size of the coarse grain zone in the HAZ and the weld metal is typically in the range of about 50 – 100 µm.[17]

3.2 A quick guide to the *J*-integral tool in LS-PrePost

The *J*-integral tool in LS-PrePost is accessed via the top menu bar: Application>Tools>*J*-integral. Both the LS-DYNA keywordfile and the **d3plot** results must be loaded into LS-PrePost for the tool to work properly, since for example material properties will be read from the keyword file. Also, the tool will automatically recognize if residual stresses need to be considered, by the presence of ***INITIAL_STRESS** and ***INITIAL_STRAIN** – keywords.

In order to calculate the *J*-integral, the user first defines the crack tip node(s), (single node in 2D, all nodes along the crack front in 3D). This is done using the general selection assistant of LS-PrePost, which makes it possible to select crack front nodes by propagating along an edge, or from a node set pre-defined in the keywordfile, which can be very convenient for 3D geometries. The next step is to select a node on the crack surface. This, in combination with the crack opening direction, will define the crack propagating direction, used in the VCE-based calculations. Finally, the user specifies the number of contours for *J*-integral computation. The contours are generated automatically by LS-PrePost: the first contour will be the elements neighboring to the crack tip node(s), and after that, the contour $k + 1$ will be the elements neighboring to contour k. It is left to the user to verify that the contours defined by this rule make sense.

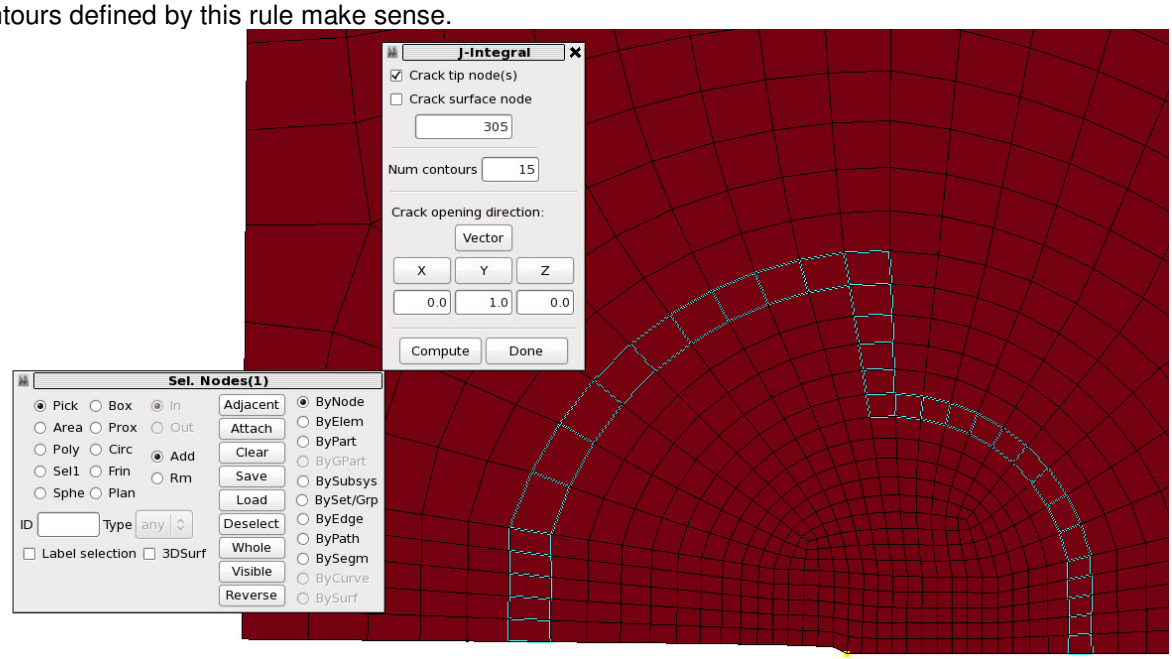

Fig.2: Example of the J-integral GUI in LS-PrePost. The highlighted elements form contour 15.

Documentation of the tool is also available from within LS-PrePost, under Help>Application>J integral.

4 Numerical examples

In this section, some examples of *J* computed by LS-PrePost from LS-DYNA simulations in both 2D and 3D are presented.

4.1 Tensile loading of a single edge notched specimen with residual stresses

A single edge notched specimen (SENT) with residual stresses, similar (but not identical) to the set-up of Ref. [1], was studied in 2D (plane strain). The geometry is described in Fig.4:. Note that a symmetry model is used. In Ref. [1], the material data is presented as a power-law relation,

$$\frac{\varepsilon}{\varepsilon_0} = \left(\frac{\sigma}{\sigma_0}\right)^n \text{, with n = 5 and } \varepsilon_0 = \frac{\sigma_0}{E}.$$

The material model was implemented as **`MAT_103`** in LS-DYNA using a smooth hardening curve, with E = 210 GPa, $\sigma_0 = 420$ MPa and Poisson's ratio ν = 0.3. The reference load [1]

$$P_0 = \frac{2}{\sqrt{3}}\left[1 - \frac{a}{w} - 1.2\left(\frac{a}{w}\right)^2 + \left(\frac{a}{w}\right)^3 + 22\left(\frac{a}{w}\right)^3\left(0.5 - \frac{a}{w}\right)^2\right] w\sigma_0 = 7.5252\,\text{kN},$$

corresponding to the limit load of a SENT specimen under plane strain conditions, was used to normalize the loading.

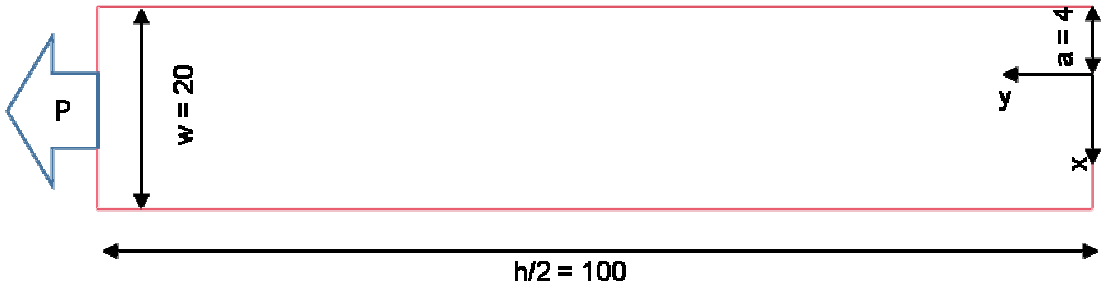

Fig.3: The geometry and loading of the SENT specimen. y-symmetry is imposed for $x \geq 0$.

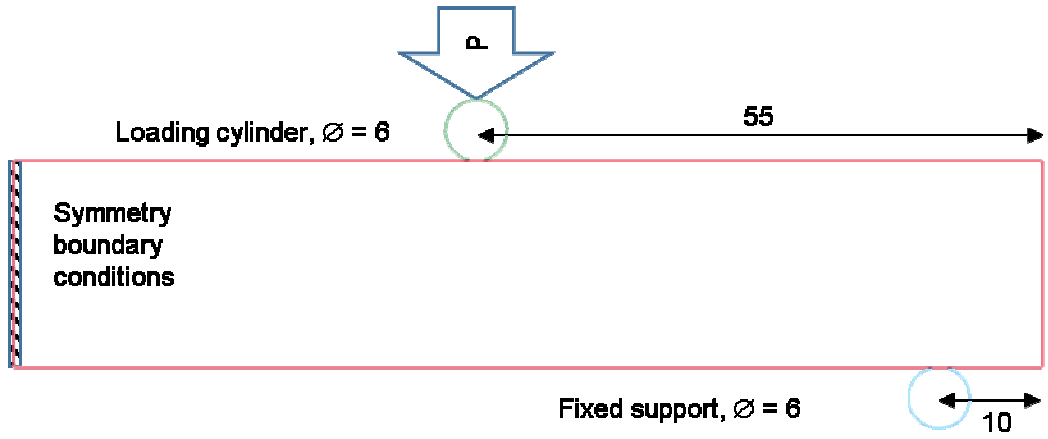

Fig.4: The four-point bending load case. A symmetry model was used.

Initially, a version of the cracked specimen with purely elastic material, subjected to tensile loading, was studied, in order to compare the elastic *J* results to the handbook solution for *K* of Ref. [6]. Eq. (3) is used for converting between *J* and *K*. The agreement is good, see Fig.5:.

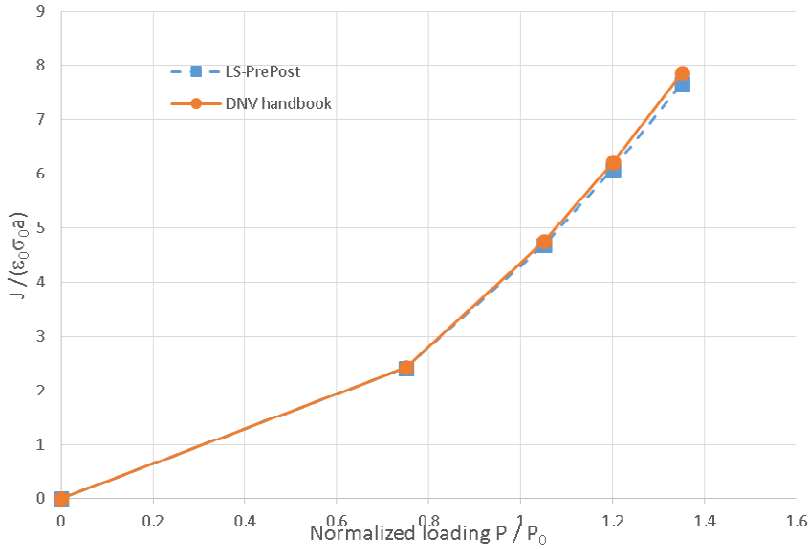

Fig.5: Comparison of J results for elastic material to handbook results [6]

In the following, the evaluation of *J* from the SENT specimen with residual stresses is described. First, the un-cracked specimen was subjected to four-point bending, by P = 1.3179 kN (see Fig.4:) and un-loaded, in order to introduce a residual stress field. The resulting variation of σ_{yy} along the line $y = 0$ is shown in Fig.6:. The residual stresses and deformation were imported to the following analysis using a **`dynain`** – file (created by **`*INTERFACE_SPRINGBACK_LSDYNA`** in the four-point bending analysis). The crack was created by a modified boundary condition at the symmetry line $y = 0$: the constraints

were released for a distance a ($x < 0$, see the top image of Fig.4:). The specimen was then subjected to tensile loadings of $0.75P_0$, $1.05P_0$, $1.20P_0$ and $1.35P_0$, and the J-integral calculated for 20 contours. The results are shown in Fig.7:.

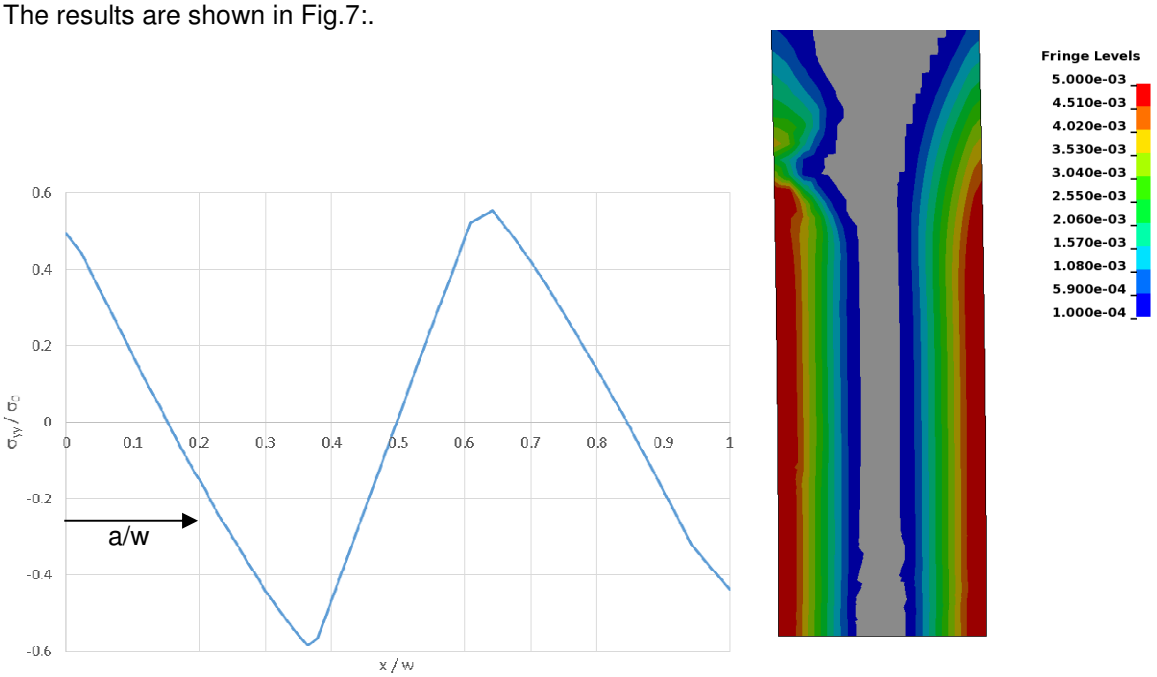

Fig.6: Residual stress after four point bending: The left image shows the normalized Y-stress along the symmetry line of the SENT – specimen. The right image shows a contour plot of the accumulated effective plastic strain.

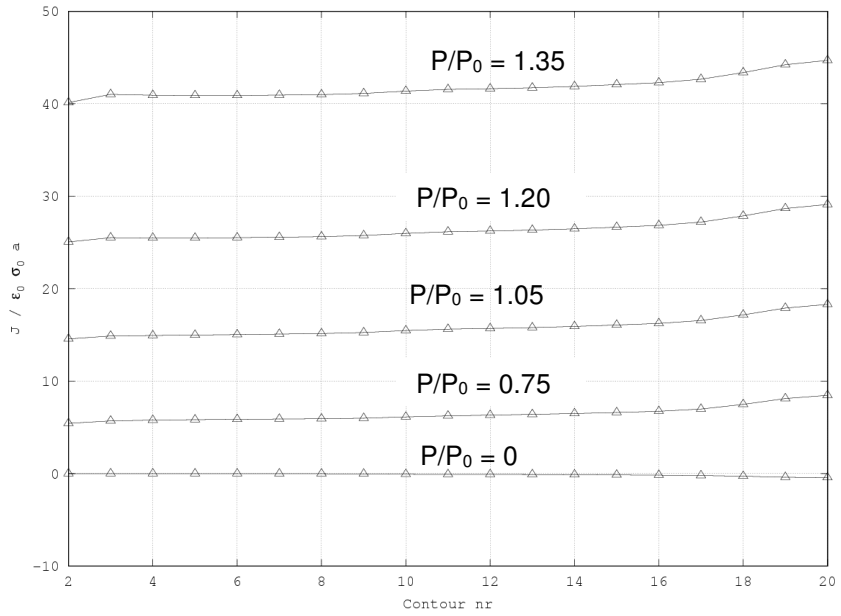

Fig.7: Normalized J-value as a function of contour number for different normalized loadings.

The J results for the SENT specimen with residual stresses from four-point bending as a function of the loading is shown in Fig.7: The J results are found to be contour-independent within reasonable accuracy. Reasons for the deviations between the ideally straight lines corresponding to perfect contour-independence and the obtained results may be that

- the numerical precision of the strain field effects the results, since it is interpolated from the element centroids rather than evaluated from the integration points directly, and
- LS-DYNA uses a large-strain formulation, which has been reported [2] to cause increased contour-dependence in cases without residual stresses.

4.2 Compact tension specimen

Results for two similar compact tension – C(T) – specimen are compared to previous results, for both 2D [2][4] and 3D [3] analyses. The calculated *J* results are also compared to the evaluation method of the ASTM standard E1820-13 [11], where *J* is evaluated from the global force-displacement curve as

$$J = J_{el} + J_{pl} = \frac{K^2\left(1-\nu^2\right)}{E} + \frac{\eta}{B_N b_o}\int_0^{\delta_{pl}(P)} P\mathrm{d}\delta_{pl} \ . \tag{11}$$

The dimensions of the first C(T) – specimen are shown in Fig.8:. The thickness is B_N = 25 mm and the remaining ligament is b_0 = 21.5 mm. The hardening curve is shown in the top image of Fig.9:. A Poisson's ratio of 0.3, and a Young's modulus of 213 GPa was used.

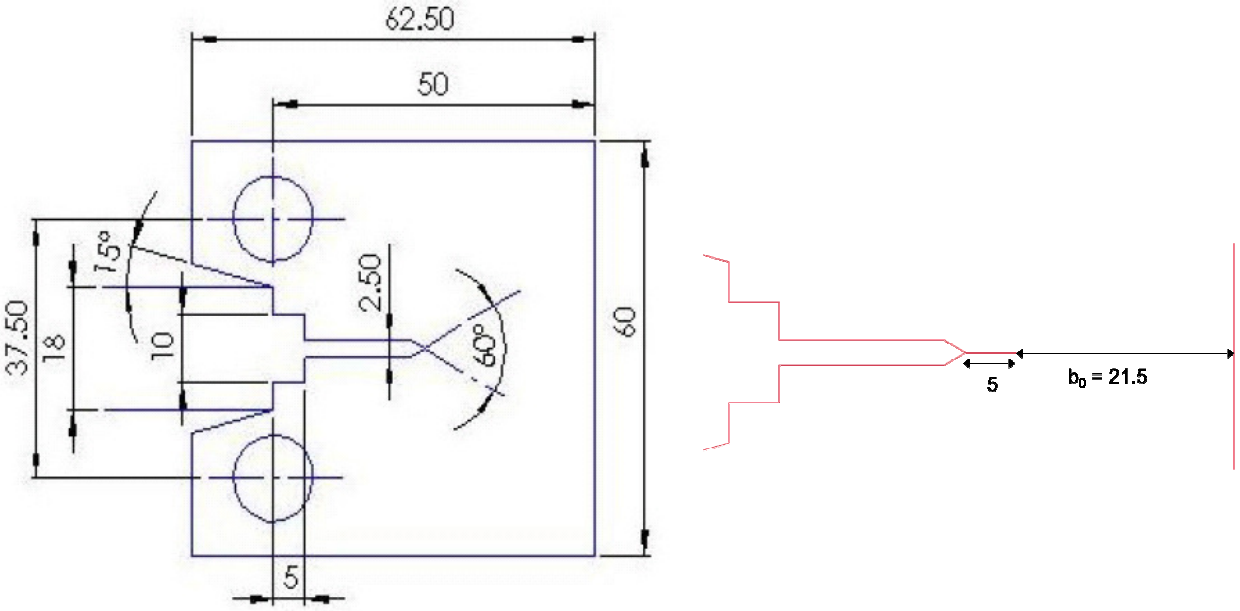

Fig.8: The left image shows the C(T) specimen geometry (from Ref. [4]). The thickness of the specimen is B_N = 25 mm. The right image shows the details of the crack length.

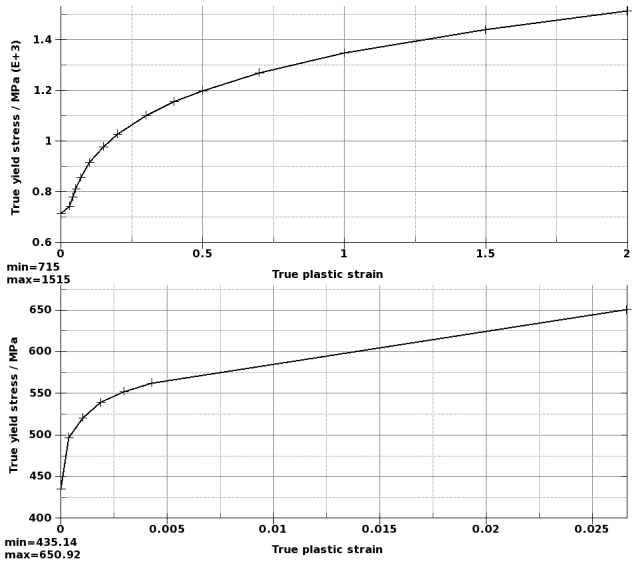

Fig.9: The top image shows the hardening curve of the material used in LS-DYNA for the analysis of the first C(T) specimen. The bottom image shows the hardening curve of the analysis of the second C(T) specimen. NOTE! Different scales on the abscissa!

The *J* vs. displacement results for the first C(T) – specimen are compared in the left image of Fig.10:. The *J* results computed by LS-PrePost are within reasonable agreement (max relative difference 9 %)

to the results obtained by the ASTM evaluation method of Eq. (11). Also, the 2D results from LS-PrePost are within reasonable agreement to the previously presented results of Refs. [2], [4].
The variation of the *J* – integral along the crack front of the 3D geometry, at a load line displacement of 1.94 mm, is shown in Fig.11:. Due to plane stress effects at the crack tips, the local *J* – value decreases towards the surface of the specimen, which also explains why *J* from the 3D model is lower than from the 2D plane strain analyses (compare Fig.10:, where the right image shows how material is being "pulled" towards the center of the specimen).

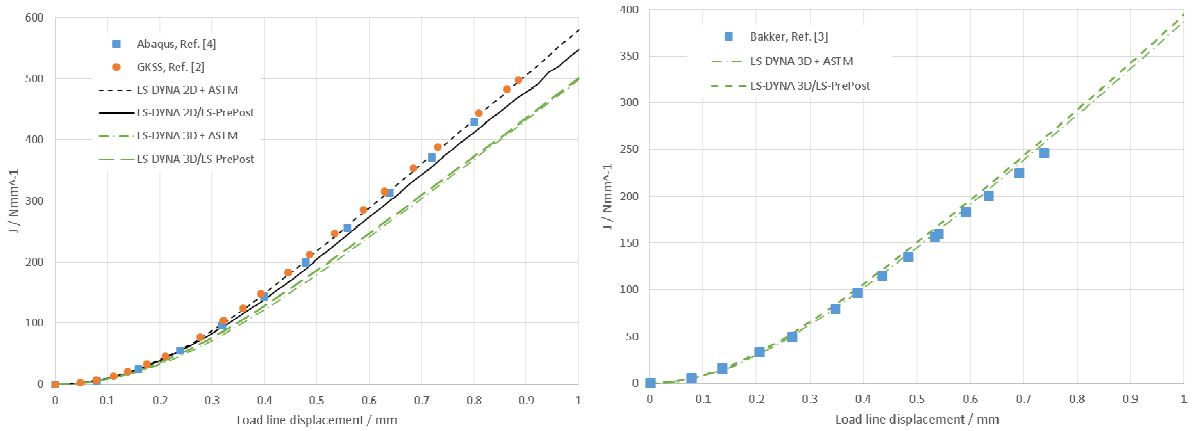

Fig.10: Left: Results comparison for the first C(T) specimen. Both 2D and 3D results. Right: Results comparison for the second C(T) specimen.

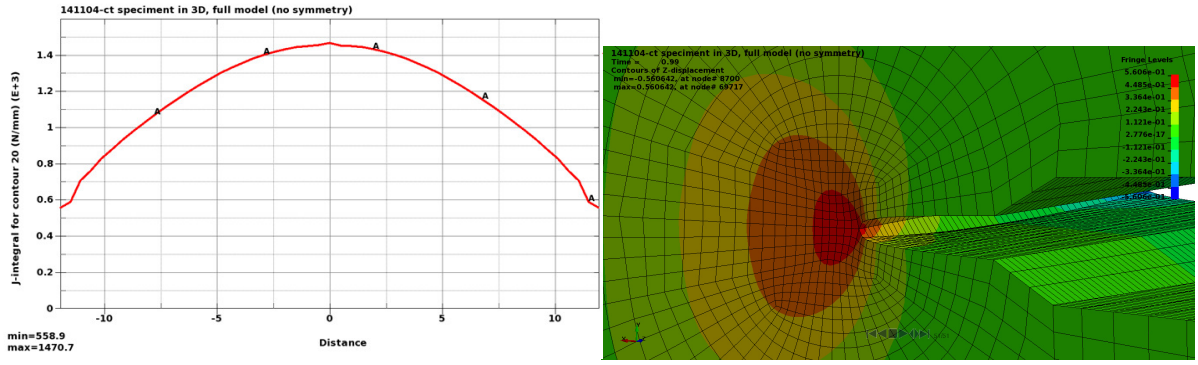

Fig.11: The left image shows the variation of the J-integral along the crack front at a load line displacement of 1.94 mm. The right image shows a fringe plot of the Z-deformation.

The geometry of the second C(T) – specimen is only slightly modified compared to the first one: the width is increased to B_N = 25.2 mm and the remaining ligament is decreased to b_0 = 20.2 mm. However, a completely different material is used, see the bottom image of Fig.9:.The results are compared in the left image of Fig.10:. Also for the second C(T) specimen, the results from LS-DYNA / LS-PrePost are within reasonable agreement to both the results obtained from the global force-displacement curve by the ASTM – method, and to the previously presented results of Ref. [3] .

4.3 A surface crack in a weld

Two different versions of a surface crack in a weld were studied subjected to tensile loading perpendicular to the crack, see Fig.12:. The first crack version represents the theoretical situation one might encounter in a design drawing, i.e., a perfect geometry with nil WRS distribution and magnitude. The second crack represents a situation in which the crack formed at room temperature during completion of the weld metal's solidification process [17]. The yield strength of the weld material is 323 MPa, and 275 MPa for the base material. Linear hardening is used with a hardening modulus of 2.22 GPa for both materials. For both materials, E=192 GPa and Poisson's ratio ν = 0.3. In the first version, the virgin materials are studied, that is without any residual stresses from the welding process. The crack is 5.875 mm deep and 38 mm wide. In the second version, the residual stresses from the welding process are included. The crack dimensions are similar to the first version, with a depth of approximately 6 mm and a width of 38 mm.

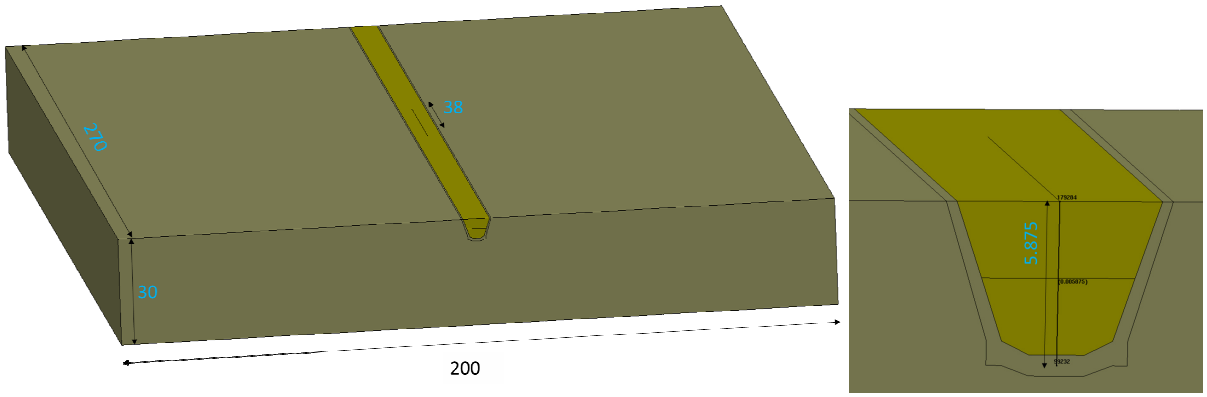

Fig.12: The geometry of version 1, with virgin material. The yield strength of the base material (brown) is 275 MPa, and the yield strength of the weld material (yellow) is 323 MPa. The right image shows a cut view through the crack, showing the crack depth

The CTOD is measured as the displacement between two nodes just above the crack tip at the center plane of the crack, see Fig.13:. Results for local J at the center plane of the crack, evaluated from contour number 7, are compared to J-values estimated from CTOD, in Fig.14: for version 1 and Fig.15: for version 2. Eq. (4) was used for estimating J from CTOD, with $m = 1.31$ (constant) and $\sigma_Y = 323$ MPa. This is a reasonable value for m, compared to for example Ref. [19], where $1.2 < m < 4$ is reported for a center cracked panel under plane strain conditions, and to Ref. [18], where $0.8 < m < 5$ is reported for a center crack in a specimen with a weld.

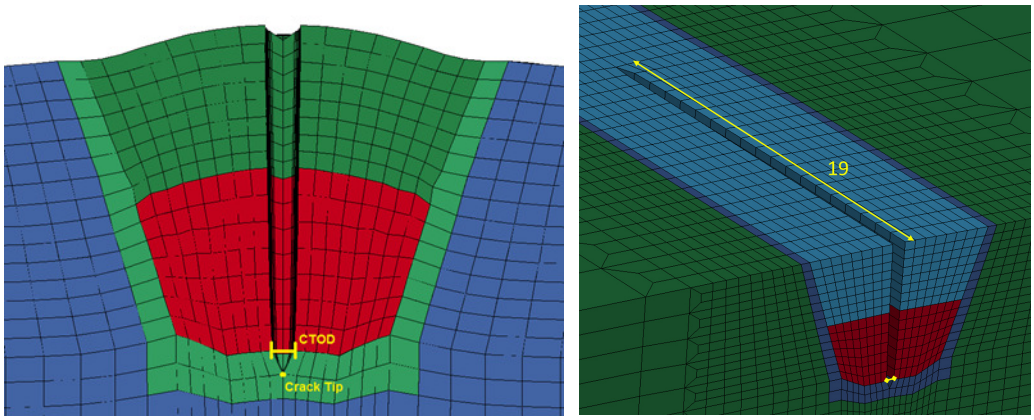

Fig.13: Illustration of the crack tip node and the location of the nodes used to measure the CTOD

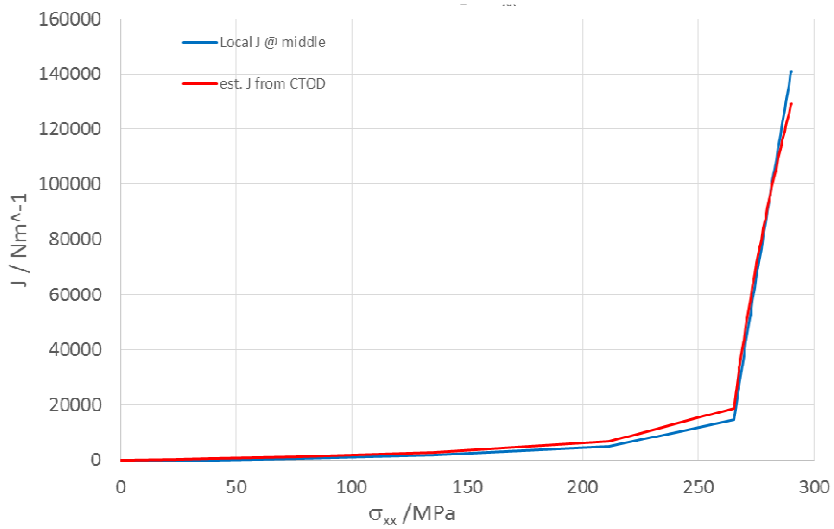

Fig.14: Local J at the center plane of the crack compared to J estimated from CTOD, as a function of the average stress, for version 1

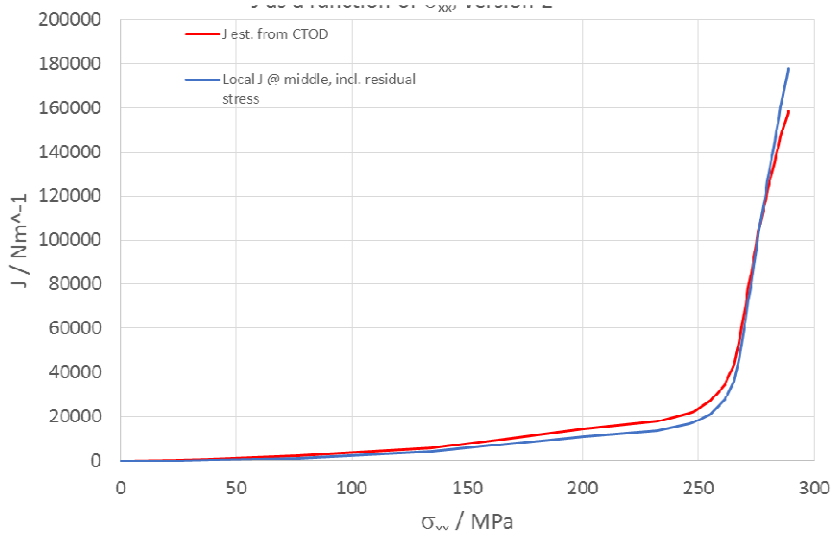

Fig.15: Local J at the center plane of the crack compared to J estimated from CTOD, as a function of the average stress, for version 2.

From Fig.14: and Fig.15:, it is concluded that the calculated *J*-value from LS-PrePost is within reasonable agreement to the *J*-values estimated from CTOD using Eq. (4). However, a quite strong contour dependence of the global *J* at the final loading is found, see Fig.16:.

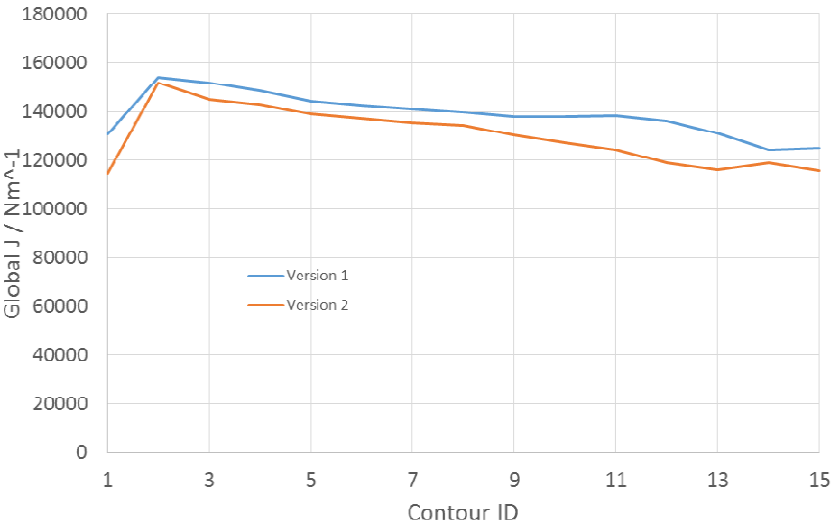

Fig.16: Contour dependence for global J for the two versions

It shall be noted that the interface between the base and weld materials is not treated correctly in the evaluation of the *J*-integral in LS-PrePost, which can be a factor of error in the presented *J* results.

5 Summary

Crack driving force (CDF) analyses in weld induced residual stress and strain fields has been found feasible by the use of the LS-DYNA CWM material models. The computation of the *J*-integral in LS-PrePost from LS-DYNA simulation results has been implemented, with a user friendly graphical interface. The numerical examples demonstrate reasonably good agreement to handbook solutions, previously published results and alternative evaluation methods.

The *J*-integral evaluation capability opens for new possibilities to use LS-DYNA within fields where classical fracture mechanics is applied for assessment of structural integrity, for example the nuclear industry, the offshore industry, and general pressure vessel design.

It remains to extend the implementation to also account for higher order solids (20/27 noded hex elements), thermal loadings and material interfaces.

6 Literature

[1] Lei, Y., O'Dowd N. P., and Webster, G. A., Fracture mechanics analysis of a crack in a residual stress field, International Journal of Fracture, 106, 2000, 195-216.

[2] Brocks, W., Scheider, I., Numerical aspects of the path-dependence of the J-integral in incremental plasticity, Technical Note GKSS/WMS/01/08, 2001

[3] Bakker, A., The three-dimensional J-integral, PhD Thesis, TU Delft, 1984

[4] Abaqus Technology Brief, Fracture mechanic study of a compact tension specimen using Abaqus/CAE, Simulia TB-04-FMCAE-1, 2007

[5] Nilsson, F., Fracture mechanics – from theory to applications, KTH (Royal institute of technology) textbook publication, 2001

[6] Recommended practice DNV-RP-F108, Fracture control for pipeline installation methods introducing cyclic plastic strain, 2006

[7] LS-DYNA Keyword User's manual version 971, Volume I – II, Livermore Software Technology Corporation (LSTC), Livermore CA, 2014

[8] Ohashi, Y., *et al.*, Verification of J-integral capability in Sierra Mechanics, Sandia report SAND2012-8720, Sandia National Laboratories, 2012

[9] BS7910, "Guide to methods for assessing the acceptability of flaws in metallic structures", ISBN: 9780580743344, BSI Standards Limited, UK, 2013

[10] Kudari, S. K., et al., On the relationship between J-integral and CTOD for CT and SENB specimens, Frattura ed Integrità Strutturale, 6, 2008, 3-10

[11] ASTM Standards, Standard test method for measurement of fracture toughness, ASTM E1820-13, American Society for Testing and Materials, Philadelphia 2013.

[12] ASTM Standards, Standard test method for plane-strain fracture toughness of metallic material, ASTM 399-90, American Society for Testing and Materials, Philadelphia 1997.

[13] Rice, J. R., A path independent integral and the approximate analysis of stress concentration by notches and cracks, Journal of Applied Mechanics, 35, 1968, 379-386.

[14] Kuna, M., Finite elements in fracture mechanics: Theory – Numerics – Applications, Springer, 2013.

[15] Kikuchi, M., and Miyamoto, H., Evaluation of JK integrals for a crack in multi-phase materials, Recent research on mechanical behavior of solids, 1, 1982, 74-92.

[16] Parks, D. M., "Virtual crack extension: a general finite-element technique for J-integral evaluations", Proc. 1st Int. conf Numerical methods in fracture mechanics, Swansea (UK), 1978, 464-478.

[17] Lindström, P., Improved CWM platform for modelling welding procedures and its effects on structural behaviour, Doctoral thesis, University West, Trollhättan, Sweden, 2015.

[18] Shih, Y., et al., Finite element analysis on relationships between the J-integral and CTOD for stationary cracks in welded tensile specimens, International Journal of Pressure Vessels and Piping, 75, 1998, 197-202.

[19] Shih, C. F., Relationships between the *J*-integral and the crack opening displacement for stationary and extending cracks, Journal of the Mechanics and Physics of Solids, 29, 1981, 305-326.